

SEISMIC FORCES ACTING ON BRIDGE SUPPORTS

Yozo Ohchi¹⁾

SUMMARY

In this report we present two kinds of approximate formulas for the seismic forces acting on the bridge supports. One of which is based on the traditional theory and the other is that of the impulse theory. The results of numerical experiments show that the seismic forces acting on the bridge support estimated by these formulas have only 10% difference from figures calculated by the modal analysis, and these forces come up more than the weight of the super-structure.

There were considerable damages of bridge structures in the "Miyagi-ken-oki" earthquake, June 12th, '78. According to the official report, the focus of this earthquake located at about 60km far away from land and 30km under the seabed. The magnitude was 7.4, and the maximum acceleration was from 250 to 300gal at the distance 100km far from the epicenter. The location of this shock is shown in Fig.1 together with the other same magnitude shocks broken out recently, and response spectra made of the shock of concerned are shown in Fig.2 normalized the maximum acceleration by 100gal. Certainly the scale of this shock was large and the shape of the response spectra were different from that of the other shocks in point of having two peaks, namely 0.3 and 1.0sec. But it is unusual that there were much more damages of bridge structures than those on the shocks broken out in the past, for example "Fukui" earthquake (1948, magnitude 7.3) or "Niigata" earthquake (1964, magnitude 7.5).

Fig.3 and 4 show the percentages of the damaged bridge shoes as against the surveyed about 3500 pieces which located within 150km of the epicenter. These figures are the only one example for many bridge damages. In addition to this, a great many of prestressed concrete poles for an electric train buried into bridge slabs were destroyed, and many of sub-structures were ruptured by this shock. Moreover, to say the super-structure, there happened the buckling of upper laterals of a Langer bridge, the rupture of upper chord members of a steel truss bridge, the cracking of a reinforced concrete bridge and so on.

The reason being subjected such a great deal damages seems that the shocked area is a center of the north-east part of Japan. So, many kind of structures have been constructed, and a good deal of those are in a time of replacement. Moreover, new constructions such as high way or rail way roads are progressing too. But it is necessary to investigate that not only old structures but also new ones were damaged by this shock. We, from the experience for the survey of earthquake damages in the past, have being confident that structures are broken down with not a vibration but an impulse at least in the case of the shock near from a focus. In the following, we will discuss this problem.

1) Professor, Dr. Eng., Hosei University, Japan

IMPULSE THEORY

For the sake of simplicity, let us consider a two-mass-system as shown in Fig.5. The equations of motion of the system may be written as follows

$$\begin{vmatrix} m_1 & 0 \\ 0 & m_2 \end{vmatrix} \begin{vmatrix} x_1 \\ x_2 \end{vmatrix} + \begin{vmatrix} c_{11} & c_{12} \\ c_{21} & c_{22} \end{vmatrix} \begin{vmatrix} x_1 \\ x_2 \end{vmatrix} + \begin{vmatrix} k_1+k_2 & -k_2 \\ -k_2 & k_2+k_3 \end{vmatrix} \begin{vmatrix} x_1 \\ x_2 \end{vmatrix} = - \begin{vmatrix} m_1 \\ m_2 \end{vmatrix} \ddot{x}_e \quad (1)$$

or $\vec{M}\ddot{\vec{X}} + \vec{C}\dot{\vec{X}} + \vec{K}\vec{X} = -\vec{M}\ddot{x}_e$

Integrating Eq.1 by the step-by-step method, we may get response displacements x_1, x_2 . But it is much easier to deal with the equations of motion in a spectrum field than in a time field. The Fourier transform of Eq.1 is

$$[K - i\omega C - \omega^2 M]X^* = -\vec{M}\ddot{x}_e^* \quad DX^* = -\vec{M}\dot{x}_e^* \quad (2)$$

where i is a symbol of the imaginary unit, D is a dynamic stiffness and X^* or x_e^* is a complex Fourier transform of a response displacement vector or a seismic acceleration. Meanwhile a Fourier transform of a response velocity vector V^* and a seismic velocity v_e^* may be written as

$$V^* = -i\omega X^* \quad v_e^* = -\dot{x}_e^*/i\omega \quad (3)$$

Then solving Eq.2 with respect X^* and substituting Eq.3 into it, we have

$$X^* = -i\omega D^{-1} \vec{M} v_e^* \quad V^* = \omega^2 D^{-1} \vec{M} v_e^* \quad (4)$$

Inverse transform of Eq.4 is the response displacement and velocity in the time field.

Using the response displacement x_1, x_2 , a force on the spring k_2 shown in Fig.5, is commonly calculated as follows

$$Q_s = k_2(x_2 - x_1) \quad \text{or} \quad Q_s^* = k_2(x_2^* - x_1^*) \quad (5)$$

But, in a system moving quickly, it may be better to consider as the following. Denoting a velocity and a impulse of the mass m_1 by v_1 and I_1 , the kinematic energy will be given by $m_1 v_1^2/2$ or $I_1^2/(2m_1)$. The same amount of potential energy with the kinematic energy is stored in the spring k_2 , when the mass m_2 is fixed, then

$$k_2 x_1^2/2 = m_1 v_1^2/2 \quad \text{or} \quad P_1^2/(2k_2) = I_1^2/(2m_1) \quad (6)$$

Moreover, considering the relation $I_1 = m_1 v_1$ and $P_1 = k_2 x_1$, the force acting on the spring k_2 from the side m_1 may be written as follows

$$P_1 = \sqrt{k_2 m_1} v_1 \quad \text{similarly} \quad p_2 = \sqrt{k_2 m_2} v_2 \quad (7), (8)$$

Since the force actually acting on the spring k_2 is the difference of Eq.7 and 8, We have a next expression after all.

$$Q_d = \sqrt{k_2}(\sqrt{m_2} v_2 - \sqrt{m_1} v_1) \quad \text{or} \quad Q_d^* = \sqrt{k_2}(\sqrt{m_2} v_2^* - \sqrt{m_1} v_1^*) \quad (9)$$

In order to confirm the validity of Eq.9, some simple experiments were conducted. Many kind of masses were putted on a vibrating table tied up with copper wire, and were given various amounts of shocks as shown in Fig.6. Then the velocity of the vibrating table at the moment of the rupture of the copper wires was observed. If the above expression is a correct one, the square root of the mass will be in inverse proportion to the velocity of the rupture. Not all experiments were successful because of a loosening of copper wires, frictions between the masses and the vibrating table and so on, but it seems that Fig.7 shows rightfulness of Eq.9.

APPROXIMATE FORMULAS

In the case of the two-mass-system, shown in Fig.5, it is rather simple to solve Eq.1 theoretically. Using this theoretical result, Q_s and Q_d of Eq.5 and 9 may be written as follows

$$Q_s = k_2(\beta_1 D_1 + \beta_2 D_2) \quad Q_d = \sqrt{k_2}(\bar{\beta}_1 V_1 + \bar{\beta}_2 V_2) \quad (10), (11)$$

moreover, if we introduce the Housner's response velocity spectrum S_v , the maximum value of Q_s and Q_d becomes as

$$Q_{smax} = k_2 \frac{\beta_1}{w_1} S_v \sqrt{1 - \delta\alpha + \alpha^2}, \quad Q_{dmax} = \sqrt{k_2} \bar{\beta}_1 S_v \sqrt{1 - \delta\bar{\alpha} + \bar{\alpha}^2} \quad (12), (13)$$

The details of the symbols in the above expression are shown in appendix.

Now, consider a problem which will do well the usage of the above mentioned expression in all case of the system having much more masses than two. As an example, let us adopt a model shown in Fig.8 and estimate the spring force between joint 2 and 3. Denoting the displacements of joints on the left side of joint 2 by X_1 and on the right side of joint 3 by X_4 , and provided that masses are lumped on joints and dampings are neglected, Eq.2 may be written as follows

$$\begin{vmatrix} D_{11} & K_{12} & 0 & 0 \\ K_{21} & D_{22} & K_{23} & 0 \\ 0 & K_{32} & D_{33} & K_{34} \\ 0 & 0 & K_{43} & D_{44} \end{vmatrix} \begin{vmatrix} X_1 \\ X_2 \\ X_3 \\ X_4 \end{vmatrix} = - \begin{vmatrix} \bar{M}_1 \\ \bar{M}_2 \\ \bar{M}_3 \\ \bar{M}_4 \end{vmatrix} \ddot{x}_e \quad (14)$$

Eliminating X_1, X_4 from Eq.14, we get

$$\begin{vmatrix} D_{22} & K_{23} \\ K_{32} & D_{33} \end{vmatrix} \begin{vmatrix} X_2 \\ X_3 \end{vmatrix} = - \begin{vmatrix} M_2 - K_{21} D_{11}^{-1} \bar{M}_1 \\ M_3 - K_{34} D_{44}^{-1} \bar{M}_4 \end{vmatrix} \ddot{x}_e \quad (15)$$

where $\bar{D}_{22} = D_{22} - K_{21} D_{11}^{-1} K_{12}$, $\bar{D}_{33} = D_{33} - K_{34} D_{44}^{-1} K_{43}$, $D_{ij} = K_{ij} - w^2 M_{ij}$

Expanding D_{11}^{-1} and D_{44}^{-1} in a series and taking the first two terms, we have

$$D_{11}^{-1} = K_{11}^{-1} (E + w^2 M_{11} K_{11}^{-1}), \quad D_{44}^{-1} = K_{44}^{-1} (E + w^2 M_{44} K_{44}^{-1}) \quad (16)$$

Then \bar{D}_{22} and \bar{D}_{33} of Eq.15 become as follows

$$\begin{aligned} \bar{D}_{22} &= \bar{K}_{22} - w^2 \bar{M}_{22} \quad \text{where } \bar{K}_{22} = K_{22} - K_{21} K_{11}^{-1} K_{12}, \quad \bar{M}_{22} = M_{22} + K_{21} K_{11}^{-1} M_{11} K_{11}^{-1} K_{12} \\ \bar{D}_{33} &= \bar{K}_{33} - w^2 \bar{M}_{33} \quad \text{where } \bar{K}_{33} = K_{33} - K_{34} K_{44}^{-1} K_{43}, \quad \bar{M}_{33} = M_{33} + K_{34} K_{44}^{-1} M_{44} K_{44}^{-1} K_{43} \end{aligned} \quad (17)$$

So, it is concluded that Eqs.14,15 may be able to use as approximate expressions for the force on the spring k_2 of Fig.5, if we use actual frequencys for w_1 and w_2 , and replace k_1, k_3, m_1 and m_2 of Eq.1 with the figure shown as followings.

$$k_1 = \bar{K}_{22} - k_2, \quad k_3 = \bar{K}_{33} - k_2, \quad m_1 = \bar{M}_{22}, \quad m_2 = \bar{M}_{33} \quad (18)$$

At last, it is noticed that $\bar{K}_{22}, \bar{K}_{33}, \bar{M}_{22}$ and \bar{M}_{33} in Eq.17 and 18 will be interpreted as the following. If we imagine the model of Fig.8(a) to be cut by the joint 2 and 3 and to be displaced at those joints by just a unit length in the direction of the vibration, we see that the forces which are necessary for this displacement are $\bar{K}_{22} - k_2$ and $\bar{K}_{33} - k_2$ (see Fig.8(b)). Next, if we suppose that every joint is subjected a force as many as its mass multiplied by its displacement for the state described above and the joint 2 and 3 are fixed, we see that the reaction at the supports are \bar{M}_{22} and \bar{M}_{33} (see Fig.8(c)).

SIEMIC FORCES ACTING ON BRIDGE SUPPORTS

It is not so difficult to solve the equations of motion for the whole bridge using the displacement method. We made a study of our problem by this method in the early stage. But we could not have good results because of too many variables. Then, very simple models have been used as a subject of investigation. The one of which is shown in Fig.9, and spring constants, masses and the other dimensions adopted in this model are shown in Fig.10 which is a typical example of piers being constructed in Japan recently. As for the Housner's response velocity spectrum S_v which is used in Eq.12 and 13, a formula written in Fig.11 was taken after had checked several shapes. This formula is tangent to two straight lines. The intersection of these lines, T_0 , could be moved according to the distance from the focus of a shock because of earlier damping of higher frequency with the distance. But, as the difference of T_0 had little influence on the results, we fixed $T_0 = 0.3$ sec. On the other side, the maximum ordinate, V_0 , of this formula is in direct proportion to figures of result. Then we may increase or decrease the figure of result in accordance with the figure of V_0 .

At first, let us compare the results of the approximate formula with the modal analysis. Table 1 is this comparison providing $V_0 = 30$ kine, $H = 5$ m and $k = 30,000$ t/m

Table 1

Mg(t/gal)	2.5	5	25	50	100
Eq. 12	89.7	103.1	141.3	185.7	253.0
modal analysis	78.4	93.9	137.4	182.9	251.0

From this table, we see that the approximate formula is in good agreement with the exact analysis. We have also compared more complicated models and have got good results too, but we can not show them because of the limited space. Next, the difference of two approximate formulas are shown in Fig.12 and 13 providing $V_0 = 100$ kine and $k = 20,000$ t/m. Fig.12 is the case of pier height 5m and Fig.13 is 10m. Dotted lines, in these figures, show the results by Eq.12 and full lines are by Eq.13. From these figures, we see that the results by Eq.13 (inpulse theory) are about twice as many as that by Eq. 12 (usual theory), and that the forces acting on bridge shoe increase with the mass of the super-structure. Moreover, it seems that the forces on bridge shoes are much more ten times of the mass namely the weight of the super-structure, but it must be noticed that the maximum of Housner's spectrum V_0 is taken as 100kine which means more than 300gal of a siesmic intensity. Lastly, to see the effect of the strength of the base lateral and rotational spring, Fig.14 and 15 are presented. Both of these figures show that the forces on the bridge shoe increase with the strength of the base springs. Specially, in the case of the base lateral spring (Fig.14), it is noticed that a step is formed at the strength of the bridge shoe's spring.

CONCLUSION

Though the inpulse theory stated in this paper is an incomplete one, it is confirmed that the force by the inpulse theory is much more than that by the usual theory, and that the force on bridge shoes increase with the weight of the super-structure. The latest progress of engineering technology enable us to construct a concrete bridge having a longer span. But, in the case of a construction of such kind of the structure which follows enlargement of the weight, we must pay the greatest care of the siesmic forces.

Moreover, a high strength concrete is generally used in this kind of structure. This is a question too. Although we do not explain this matter in this paper, it is said in general that a stronger material is more brittle. This is also true in the case of a concrete, and the high strength concrete seems to be weaker against the impulse force. The stiffness of a material is important for an seismic design as well as the strength of it.

APPENDIX

$$\left. \begin{aligned} \beta_1 \\ \beta_2 \end{aligned} \right\} = \mp \frac{1}{w_2^2 - w_1^2} \left(\frac{k_3}{m_2} - \frac{k_1}{m_1} \right)$$

$$\left. \begin{aligned} \bar{\beta}_1 \\ \bar{\beta}_2 \end{aligned} \right\} = \frac{\sqrt{m_1} + \sqrt{m_2}}{2} \mp \frac{\sqrt{m_2} - \sqrt{m_1}}{2(w_2^2 - w_1^2)} \left(\frac{k_2 + k_3}{m_2} - \frac{k_1 + k_2}{m_1} - 2 \frac{k_2}{\sqrt{m_1 m_2}} \right)$$

$$\left. \begin{aligned} w_1^2 \\ w_2^2 \end{aligned} \right\} = \frac{1}{2} \left(\frac{k_1 + k_2}{m_1} + \frac{k_2 + k_3}{m_2} \right) \mp \sqrt{\frac{1}{4} \left(\frac{k_2 + k_3}{m_2} - \frac{k_1 + k_2}{m_1} \right)^2 + \frac{k_2^2}{m_1 m_2}}$$

$$D_i = \frac{1}{w_i} \int_0^t \exp[-\zeta_i w_i (t-\tau)] \sin[w_i'(t-\tau)] \ddot{x}_e d\tau$$

$$V_i = \frac{dD_i}{dt}, \quad w_i' = \sqrt{1 - \zeta_i^2}, \quad \zeta = \text{damping ratio}$$

$$\alpha = \frac{w_1 S V_2}{w_2 S V_1}, \quad \bar{\alpha} = \frac{\beta_1 S V_2}{\beta_2 S V_1}, \quad \delta = \frac{2}{1 + \epsilon^2}, \quad \epsilon = \frac{1 - \zeta^2}{\zeta^2} \left(\frac{w_2 - w_1}{w_2 + w_1} \right)^2$$

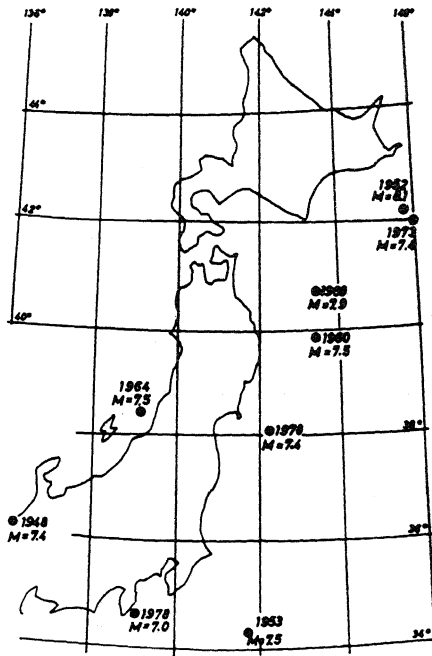


Fig. 1

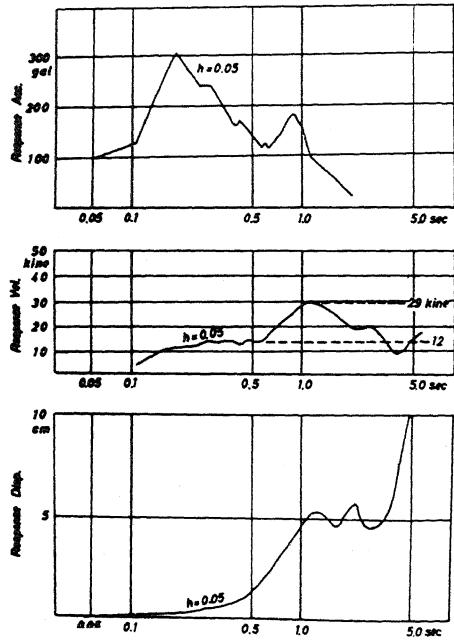


Fig. 2

Pier-Hight		<8m	8~10	10~12	12m<	Total
Bridge Type	RC-15m(FC)	28	15	12	54	26
	RC-20m(FC)	30	48	36	78	41
	PC-25m(FC)	100	43	100	88	93
	PC-30m(BP)	0	0	0	3	2
Total		25	35	33	38	33%

Fig. 3

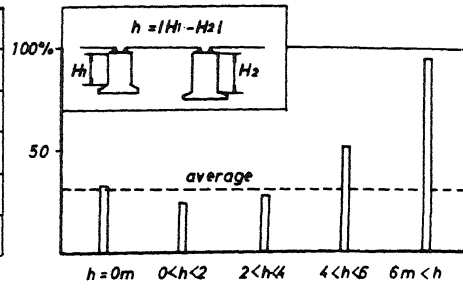


Fig. 4

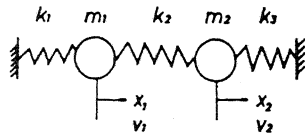


Fig. 5

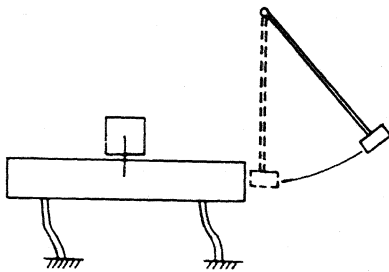


Fig. 6

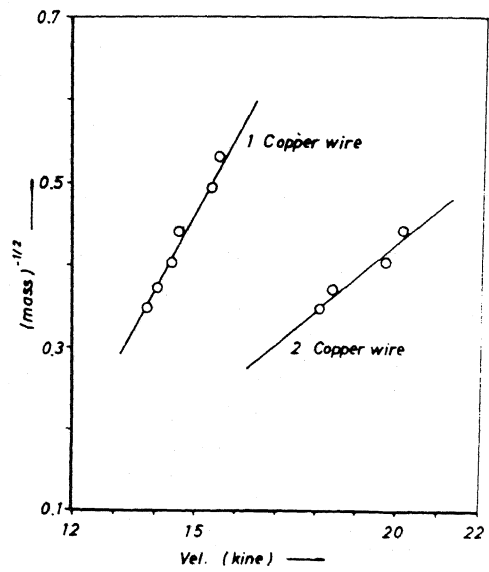


Fig. 7

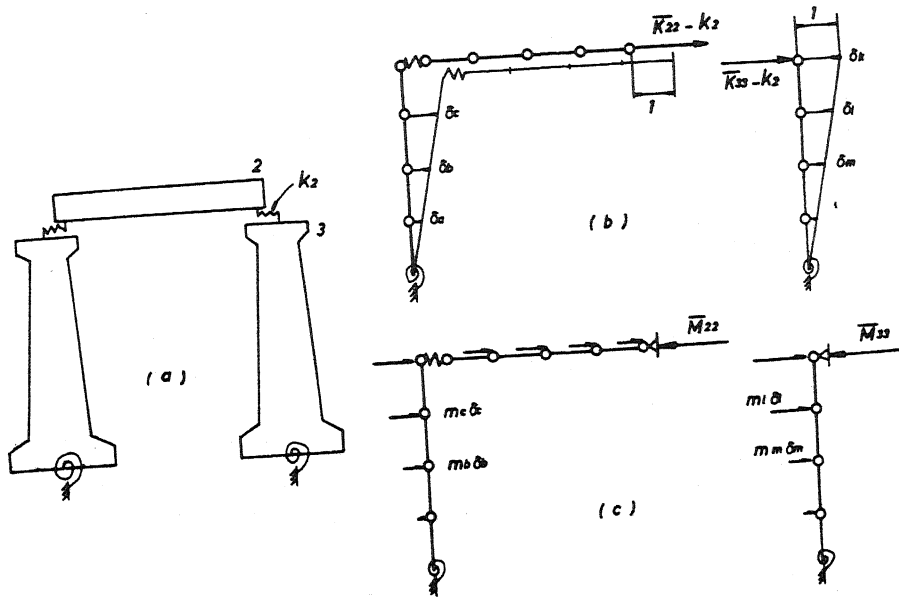


Fig. 8

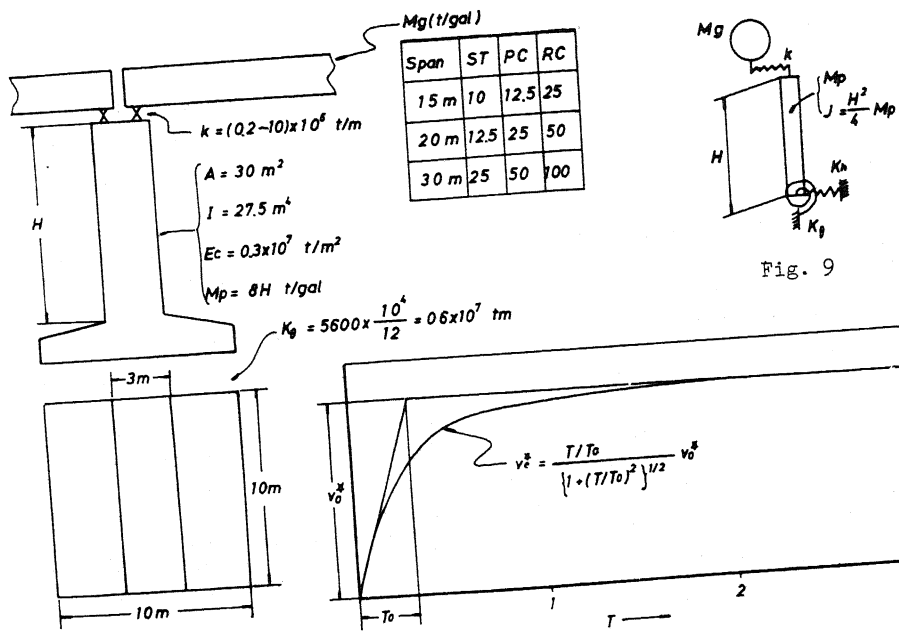


Fig. 9

Fig. 10

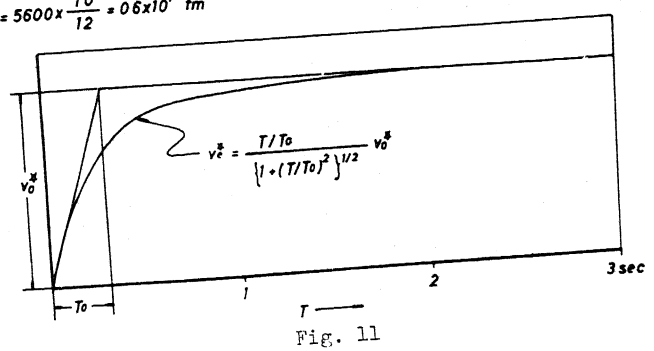


Fig. 11

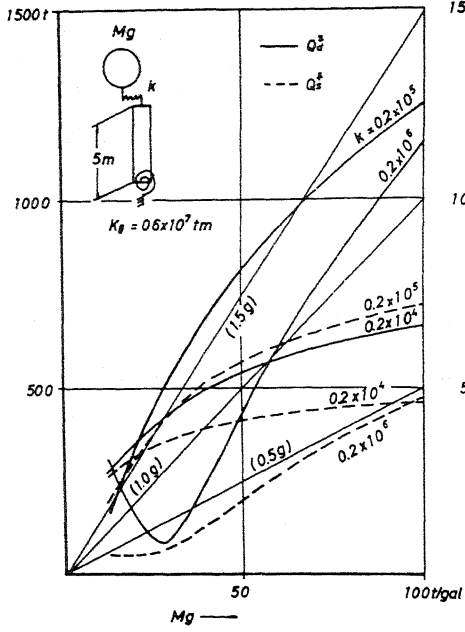


Fig. 12

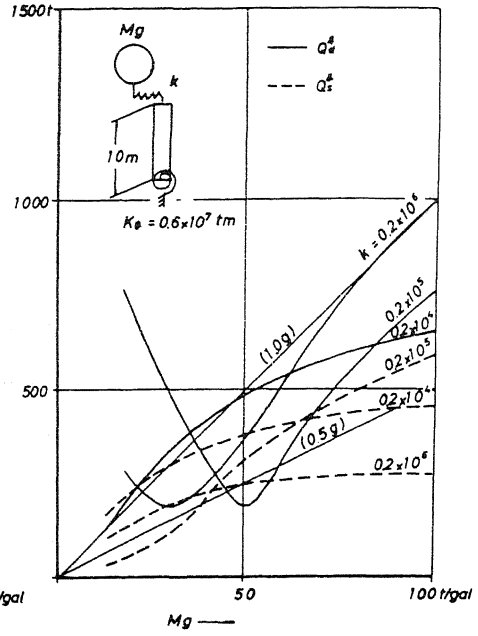


Fig. 13

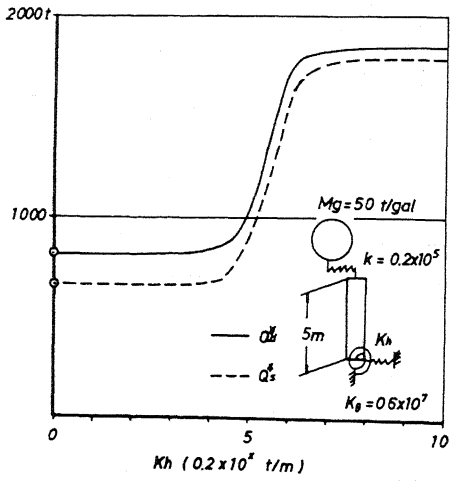


Fig. 14

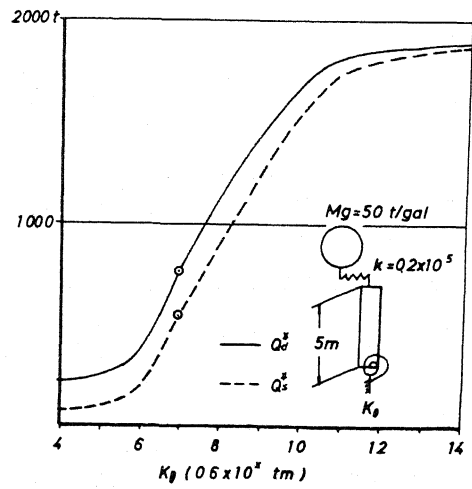


Fig. 15